

BOILING PHENOMENOLOGY USING COUPLED MAP LATTICE

Thesis
submitted in partial fulfillment of the requirements for the degree of

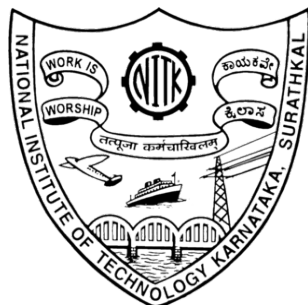
**MASTER OF SCIENCE
IN
PHYSICS**

by

Vipul Rai
(206PH030)

Under the Supervision of

Dr. Shajahan T.K.



DEPARTMENT OF PHYSICS
NATIONAL INSTITUTE OF TECHNOLOGY KARNATAKA (NITK)
SURATHKAL, MANGALORE - 575 025
June, 2022

Abstract

For boiling, a simple model is proposed using coupled map lattice (CML) method known in non-linear spatio-temporal chaos dynamics. The model was proposed by Tatuso Yanagita in 1992. In this model I am increasing temperature of a bottom plate and keeping temperature of top plate at 0° C , the model shows three successive phases; conduction, nucleate boiling and film boiling. In the nucleate regime the heat flux increases by increasing temperature of bottom plate, and heat flux decreases in the film boiling regime by increasing temperature of bottom plate, which verifies the boiling characteristic curve. Through this method, we can find out the critical heat flux point for different fluids which is very useful for industrial application (like Coal based steam power plant, Boiler etc.) To simulate boiling phenomena explicit scheme using Euler finite difference method is employed. I am using python as programming language for simulation.

Contents

1	Introduction	2
1.1	Special About Nonlinearity	2
1.2	One-Dimensional Maps	3
1.3	Chaos	3
1.4	Spatiotemporal Chaos	5
1.5	Coupled Map Lattice	6
1.6	Boiling Characteristic Curve	7
2	Review Of Literature	12
3	Methodology	14
3.1	Modeling	14
3.2	Thermal Diffusion	15
3.3	Numerical Methods	15
3.4	Creation and Floating Motion of Bubbles:	17
3.5	Latent Heat Effect :	18
3.6	Parameter Details	19
3.7	Time advancement	19
3.8	Overall Solution Algorithm	19
4	Results and Discussion	22
4.1	Thermal Diffusion Plot	22
4.2	Creation and floating motion of bubbles	23
4.3	Heat Flux	26
5	Conclusions	27
A	Appendices	28
	Appendices	28
	A Thermal Diffusion	28
	B Creation and floating motion of Bubbles	29

List of Figures

1.1	Bifurcation Diagram	4
1.2	Two trajectories started with the initial conditions $x_0 = 0.950$ (marked by solid blue line) and $x'_0 = 0.9505$ (marked by dashed line)	5
1.3	Separation distance plot of two above trajectories	5
1.4	Experimental setup by Nukiyama	8
1.5	Nukiyama's boiling curve for saturated water at 1 atm	8
1.6	Leidenfrost effect	10
1.7	Controlling Heat Flux	10
3.1	Computational Domain and Lattice	16
4.1	Diffusion Plot at time: a =90, b =450, c =950	22
4.2	$T_{bottom} = 9.75$ at time: a = 910, b = 920, c = 930, c = 940	23
4.3	$T_{bottom} = 9.85$ at time: a = 540, b = 560, c = 580, c = 600	24
4.4	$T_{bottom} = 9.92$ at time: a = 540, b = 560, c = 580, c = 600	25
4.5	$T_{bottom} = 9.96$ at time: a = 520, b = 540, c = 560, c = 580	25
4.6	T_{bottom} V/S Heat Flux	26

Chapter 1

Introduction

Here I am using nonlinear dynamics technique to understand Phenomenology of Boiling. Let's go through some background information (like nonlinearity, chaos and Spatiotemporal-Chaos) before we get into the boiling characteristic curve.

1.1 Special About Nonlinearity

A physical system whose motion is described by linear differential is called a linear system. Linear equations form an enormous set of all possible differential equations with many simple properties that are not shared by the general nonlinear equations. Linear homogeneous equations satisfy the superposition principle - that any linear combinations of solutions give us another solution. But we assume linear property carries over to nonlinear equations. *This assumption is frequently wrong. The main message about the chaos, which never appears in linear systems, is a common occurrence in nonlinear systems.*

An example of a simple pendulum : whose equations of motion are nonlinear, can exhibit *chaos*? Non-linearity is essential criteria for chaos, if a system's equation of motion is linear, it cannot exhibit chaos. But nonlinearity does not guarantee chaos. Even in the case of a simple pendulum when the amplitude is large equation of motion becomes nonlinear but never exhibits chaos. The behavior of a chaotic mechanical system can be very complicated and the need to describe this behavior has given rise to a whole array of new ways to view the motion of such a system - state-space orbit, Poincare section, bifurcation diagrams. There are a system that is complicated enough to exhibit chaos, but still simple enough not to need all these new tools for their description. In a particular, a driven damped pendulum, whose equation of motion is nonlinear, can exhibit chaos but can be described in a reasonably elementary term. In conventional dynamical equilibrium and periodic oscillations chaotic dynamics new significant additions.

1.2 One-Dimensional Maps

Here is we discuss a new class of dynamical system in which time is discrete rather than continuous. These systems are known variously as difference equations, recursion relations, iterated maps, or simply maps.

For instance, suppose if we repeatedly press the cosine button on our calculator, starting from some number x_0 . Then the successive iterations are $x_1 = \cos(x_0)$, $x_2 = \cos(x_1)$, and so on. And we set our calculator to radian mode and try it. And we see the surprising result that emerges after many iterations. The rule $x_{n+1} = \cos x_n$ is an example of a **one-dimensional map**, so-called because the points x_n belong to the one-dimensional space of real numbers. The sequence x_0, x_1, x_2, \dots is called the orbit starting from x_0 .[7]

As models of natural phenomena. In some scientific contexts it is natural to regard time as discrete. This is the case in digital electronics, in parts of economics and finance theory, in impulsively driven mechanical systems, and in the study of certain animal populations where successive generations do not overlap.

As simple examples of chaos. Maps are interesting to study in their own right, as mathematical laboratories for chaos. Indeed, maps are capable of much wilder behavior than differential equations because the points x_n hop along their orbits rather than flow continuously.

The study of maps is still in its infancy, but exciting progress has been made in the last few decades, thanks to the growing availability of calculators, then computers, and now computer graphics. Maps are easy and fast to simulate on digital computers where time is inherently discrete. Such computer experiments have revealed a number of unexpected and beautiful patterns, which in turn have stimulated new theoretical developments. Most surprisingly, maps have generated a number of successful predictions about the routes to chaos in semiconductors, convecting fluids, heart cells, lasers, and chemical oscillators.

1.3 Chaos

In the year 1963, E.N. Lorenz numerically integrated a simplified system of the three coupled first-order nonlinear equations of the fluid convection model describing the atmospheric weather conditions. [6] The bounded nonperiodic trajectories of the equations started from two nearby initial states diverged exponentially until they become completely uncorrelated resulting in the unpredictability of future states in a fully deterministic dynamical system. Such a solution became known as chaotic and, with this discovery, the field of chaotic dynamics was born. The phenomenological behavior of chaos—e.g., sensitivity to the tiniest changes in initial conditions or seemingly random and unpredictable behavior that never-

theless follows precise rules—appears in many of the models in these disciplines. For example 1-D logistic map [8] $x_{n+1} = rx_n(1 - x_n) = f(x_n)$ where $n = 0, 1, 2, 3, \dots$. Here $x_n \geq 0$ is a dimensionless measure of the population in the n th generation and $r \geq 0$ is intrinsic growth rate. We assume that $0 \leq x \leq 1$. An important characteristic property of the solutions of the logistic map for $r < r_c$ ($r_c = 3.57$) (where only periodic solutions occur) is that they are, in general, *insensitive to initial values* of x provided $0 < x < 1$. Irrespective of the initial value of x the successive iterations asymptotically approach the same periodic solution. By the numerical analysis, $r > r_c$ the sequence x_n never settle down to equilibrium point or to a periodic cycle. So the long term behavior is aperiodic. Such behavior is called **chaotic** since solution is highly sensitive to the initial conditions.[7]

To understand the sensitive dependence on initial conditions we iterate the map

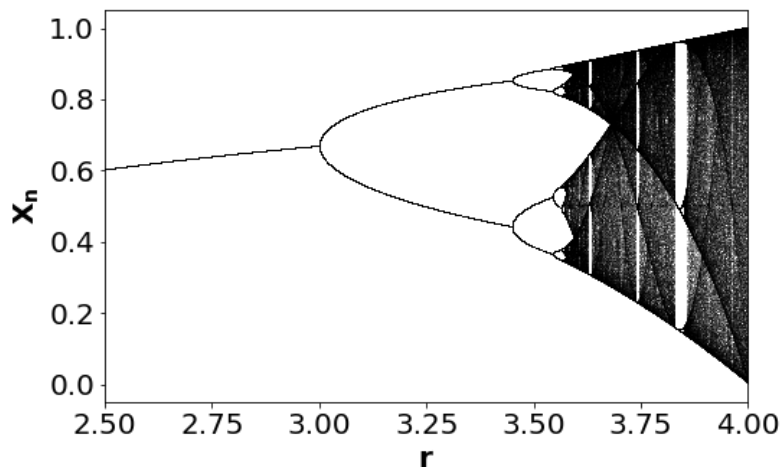


Figure 1.1: Bifurcation Diagram

with two near by initial conditions for same value of $r > r_c$ and see the difference between two resultant sequences. We see that after 8 or 9 iterations trajectories separate apart.

Separation plot $S_n = x'_0 - x_0$ between the two trajectories, S_n varies irregularly with n , so it indicate sensitive dependence of the dynamics on initial conditions. We also observe that the distance between $S_n \rightarrow \infty$ as $n \rightarrow \infty$, then at least one of the two trajectories considered must go to ∞ leading to the unbounded motion. Since separation does not go to infinity because the range of x is confined between interval $(0,1)$ i.e. it has definite boundary so the **chaotic** motion is always bounded.

Usual definition of chaos can be: “Chaos is *aperiodic long term behaviour* in a de-

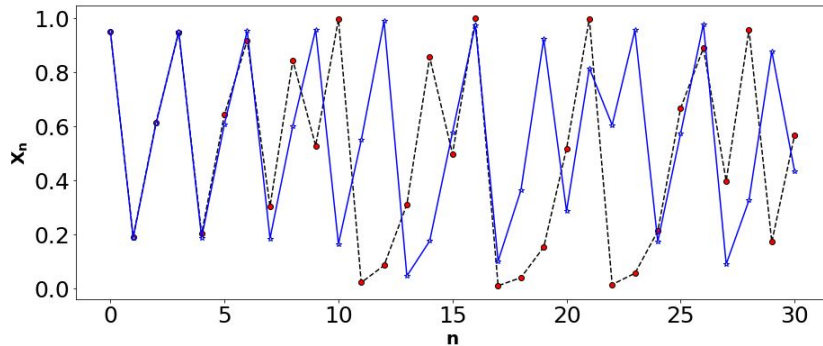


Figure 1.2: Two trajectories started with the initial conditions $x_0 = 0.950$ (marked by solid blue line) and $x'_0 = 0.9505$ (marked by dashed line)

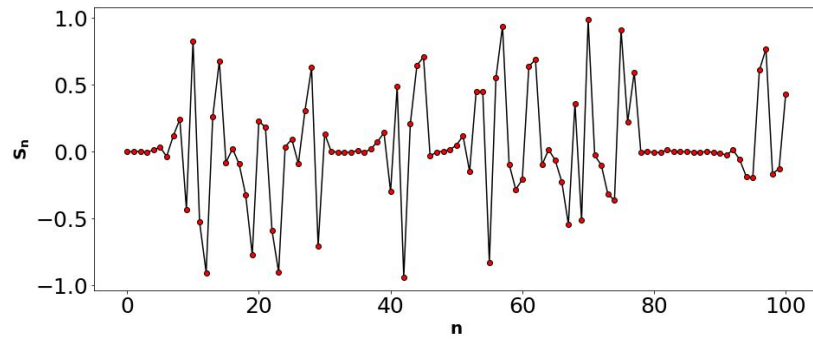


Figure 1.3: Separation distance plot of two above trajectories

terministic system that can exhibits *sensitive dependence of initial conditions*".[7] "aperiodic long term behaviour" means the trajectories do not settle down to a fixed point. "deterministic system" means that the system has no random or noisy input or parameter the irregular behaviour arises from the system's non-linearity.

Observing similar chaotic behavior in such diverse fields certainly presents a challenge to our understanding of chaos as a phenomenon.

1.4 Spatiotemporal Chaos

Chaotic systems have been studied that are not reducible to a model with a small number of degrees of freedom, even at the onset of chaos. Such systems are said to be "large" and to display "spatio-temporal chaos," because their description appears to require a large number of chaotic elements distributed in space.[1] An exciting advance in the study of spatiotemporal chaos is the development of a number of experimental systems that are well characterized and precisely controlled, and in some cases approach the ideal of large system size so that a statis-

tically homogeneous state, independent of boundary effects, seems to exist over much of the system. Such examples offer the real possibility of understanding spatiotemporal chaos by means of a combination of theoretical, numerical, and experimental techniques that have been successfully applied to the study of regular spatial patterns in non-equilibrium systems.

The rotating convection system is a representative example. The non rotating case, the familiar Rayleigh-Benard convection, has served well as a canonical system for the study of time independent spatial patterns and their transients

1.5 Coupled Map Lattice

The nonlinear dynamics and the chaos theory was successful in understanding low dimensional complex dynamics (e.g. Lorenz system and Logistic map). A new model would be necessary for higher-dimensional complex systems. The study of higher dimensional spatially extended systems has become a fascinating and challenging subject in recent years. This is due to the fact that complex systems might exhibit some unusual behaviours, such as spatiotemporal chaos, patterns formation, travelling waves, spiral waves, turbulence and so on. The control and synchronise of such behaviours have extensive and great potential of interdisciplinary applications, such as security communication, laser, many fluid dynamics, biological systems, crystal growth, information processing, chemical reactor, biochemistry, medicine and engineering.

Spatially extended systems are often modeled by partial differential equations(PDE), ordinary differential equations (ODE), cellular automata (e.g. cellular neural networks (CNNs)) and coupled map lattices (CML). Such systems are proven to be useful in studying qualitative properties of spatially extended dynamical systems. They can easily be simulated on a computer, and able to capture some essential qualitative feature of physical systems.

CML is a dynamical system with discrete time (map), discrete space (lattice)and continuous state. It consists of dynamical elements on a lattice, [4] which interact (coupled) with suitably chosen sets of other elements. They were introduced by K. Kaneko in 1983 as simple models with essential features of spatio-temporal chaos. [5]

Model	space	Time	state
PDE	Continuous	Continuous	Continuous
Coupled ODE	Discrete	Continuous	Continuous
CML	Discrete	Discrete	Continuous
Cellular Automata	Discrete	Discrete	Discrete

Modelling of physical phenomena through CML is done by following steps.

1. Choose a (set of) field variable on a lattice.
2. Decompose the phenomenon of interest independent units (e.g. convection ,reaction, diffusion etc).
3. Replace each unit by simple parallel dynamics on a lattice, where the dynamics consists of a nonlinear transformation of the field variable at each lattice point.
4. Finally carry out each unit dynamics successively.

CML equation for 1-D logistic map:

$$x_{n+1}(i) = (1 - \varepsilon)f(x_n(i)) + \frac{\varepsilon}{2}[f(x_n(i+1)) + f(x_n(i-1))]$$

Here 'n' is discrete time step and 'i' discrete lattice point ($i = 1, 2, 3, \dots, N$) where $f(x)$ is the local logistic map.

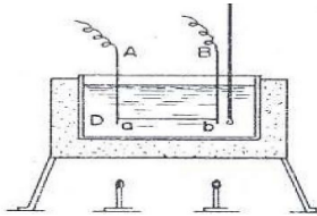
$$f(x) = 1 - rx^2$$

As shown by the basic model, the dynamics of a CML is governed by two competing terms; an individual temporal nonlinear reaction represented by f and r spatial interaction (coupling) with variable intensity ε . The coupling factor ε tries to homogenize the system while the nonlinear parameter r tries to make the system chaotic. When these parameters are varied then different patterns are formed which are the universality classes in CML model.

1.6 Boiling Characteristic Curve

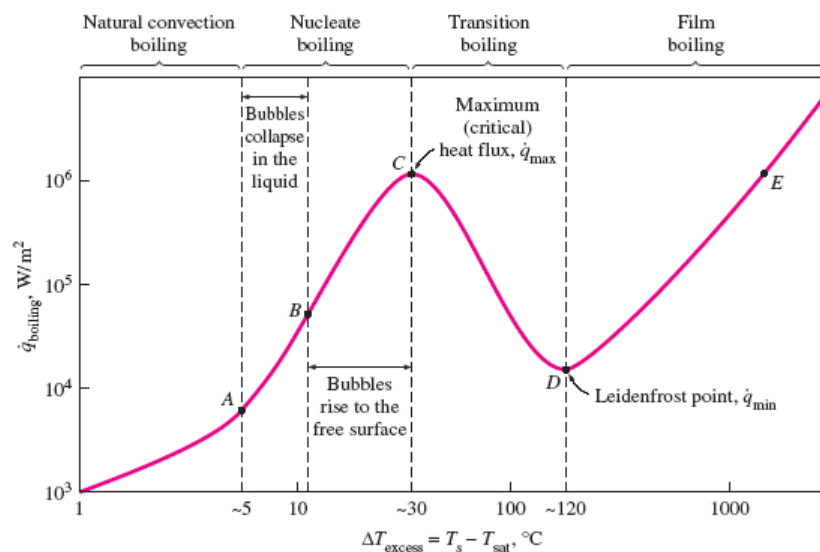
In 1934 Shiro Nukiyama was the first to identify the several stages of boiling. His experimental setup allowed him to control the heat flux 'q' by electrically controlled heater. [9] The experiments were conducted by using a nichrome wire submerged in water at atmospheric pressure, shown in Figure 1.4

His setup was power regulated, which means that the wire temperature was the dependent variable and the heat flux was the independent variable. As we supply the heat, wire temperature is increased and its resistance also changes. So we measure resistance of the wire, we also get the idea of temperature. Nukiyama noticed that the formation of bubbles occurs when the difference between the hot surface T_s and the saturated water T_{sat} is nearly five degrees. ($\Delta T_{excess} = T_s - T_{sat} \approx 5$). As

**Figure 1.4:** Experimental setup by Nukiyama

power is increased further, the heat flux jumps to very high value. Using a platinum wire, Nukiyama was able to reach heat fluxes above the critical heat flux (C) **Figure 1.5**. He assumed the graph he saw was the product of a power-controlled heating process. He also believed that if the heating process follows an independent control of the surface temperature T_s (or temperature difference (ΔT_{excess})), a missing region $C \rightarrow E$ in **Figure 1.5** would have been obtained. His hypothesis was later on confirmed by Drew and Muller, and thereby obtaining the missing portion of the boiling curve.

The boiling curve for water at atmospheric pressure is represented in Figure 1.5 It is characterized into four different regions:

**Figure 1.5:** Nukiyama's boiling curve for saturated water at 1 atm
[2]

Natural Convection : In natural convection region, liquid is at atmospheric

temperature and then we started heating process, the liquid temperature is much below the saturation temperature . So no boiling will take place but definitely heat transfer will take place. The fluid motion in natural convection is driven by the buoyancy forces within the fluid itself. “Buoyancy is due to the combined presence of a fluid density gradient and a body force (like gravitational force) that is proportional to density”. The presence of a temperature gradient induces a density gradient, as the density of fluids is temperature dependent due to expansion effects.

Nucleate Boiling : Nucleate boiling is the regime where boiling could be observed. The thermal process of nucleate boiling is particularly efficient. Because of its ability to transport a high amount of heat with a little temperature difference, it is commonly used in industrial equipment.

Isolated Bubble ($A \rightarrow B$) : The solid surface temperature T_s is more than the saturation temperature T_{sat} . So bubble are generated.

After **B** , number of isolated bubble increase by increasing the temperature and distance between two isolated bubble will decreases. Then the frequency of bubble generation will also increase. Vapour column and jet try merge together and devlop **nucleate boiling**. The heat flux in this regime strongly depends on the number of nucleation sites.

Critical Heat Flux or Burn Point (C) : In *nucleate boiling* region, at point (C) at which heat flux is maximum known, as critical heat flux or burnout point. Once we cross this point large temperature difference is required to get the same heat flux and most material may be going to burn at this temperature. Most of boiling heat transfer heater are operated below the *burnout point* to avoid that tragic result.

Transition Boiling regime ($C \rightarrow D$) : Transition boiling or the unstable film boiling regime is located at the region between the film boiling and the nucleate boiling. And this region heater surface is partially blocked by vapour patches. The vapor patches act as a thermal insulator and the heat flux will continue to reduce until the Leidenfrost point is reached, this effect known as Leidenfrost effect. (*The Leidenfrost effect, a liquid close to a surface that is significantly hotter than the liquid's boiling point, produces an insulating vapor layer that keeps the liquid from boiling rapidly.*)

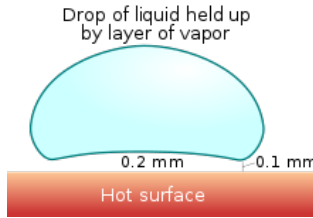


Figure 1.6: Leidenfrost effect
[11]

At the point of minimum heat flux, because of no contact between the heater surface and the liquid, the vapor blanket completely covers the heater surface. During this point, heat transfer between the heater surface and the liquid will take place by radiation and conduction through the vapor blanket. This is very unsta-

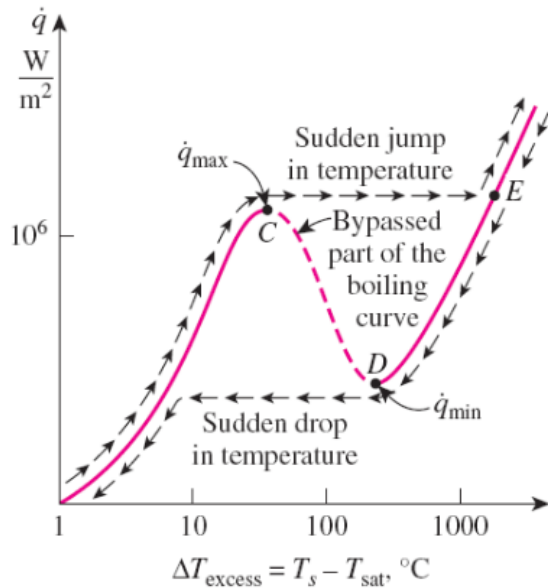


Figure 1.7: Controlling Heat Flux

ble regime and we can not record this regime, where we are unable to control the temperature i.e we are controlling heat flux. And transition region is totally bypass (*nucleate to film boiling*) in Figure 1.7. So The branch ($C \rightarrow D$) cannot be realized using usual instruments which prescribe the heat flux fed into the system.

Film Boiling($D \rightarrow E$) : The low heat transmission rates in the film boiling area are due to the presence of a vapour film between the heater surface and the liquid. Temperature of heater suddenly rises from ($C \rightarrow E$) by the insulating action of

vapor film which cover the surface of heater. The heat transfer rate increases with increasing excess temperature due to radiation to the liquid.

The heater melts when the temperature of melting point is lower than that of film boiling 'E'. For this reason, in some technical application of boiling (nuclear engineering, boiler, cooling system for superconductive magnet) one must adjust the thermal load at safety level, well below the critical heat flux 'C'. So prediction of critical heat flux is also very precise for many industrial application. Most of the industrial application point of view, avoid the film boiling regime.

Chapter 2

Review Of Literature

For boiling, a simple model is proposed by Tatsuo Yanagita using a coupled map lattice method .The model illustrates three phases as the temperature of the bottom plate rises; conduction, nucleate and film boiling. [12] [13] Ideally speaking, a computational fluid dynamics (CFD) study of pool boiling would be possible if the Navier–Stokes equations could be solved together with the continuity and energy equations along with phase change and appropriate boundary conditions. In principle, physical transport phenomena are described by the Navier-Stokes equation. [3]

$$\rho \frac{Du}{Dt} = -\nabla p + \rho \mathbf{g} + \mu \nabla^2 \vec{v} \quad (2.1)$$

Here $\frac{D}{Dt}$ is called substantial derivative or material derivative or total derivative, ρ = density, p = pressure, μ = viscosity , v = velocity and $\rho \mathbf{g}$ = external force (that act on fluid) . $\mu \nabla^2 v$ is diffusion term (For Newtonian Fluid viscosity operate as diffusion of momentum) and $-\nabla p$ tells about the fluid flows in the direction of largest change in pressure .

Unfortunately, however, the phenomenology of the heated surface and the boundary condition at the liquid–vapour interface vary in time and space in a very complicated manner and are not easy to handle. With the numerical techniques available at present, only a few bubbles at most can be dealt with.CML (coupled map lattice) has long been acknowledged as a useful tool for understanding the qualitative and basic nature of complex phenomena and has been applied to many physical systems. The CML method is based on a dynamic system with continuous field variables but discrete space and time, in which local dynamics propagates in space by diffusion or flow and time is advanced by repeated mapping. From the study of non-linear chaos dynamics it is known that a complex physical system is not always governed by a complex system of equations. Earlier studies of boiling based on non-linear dynamics, though few and recent, suggest that boiling is a

kind of spatiotemporal chaotic phenomenon. However, applications of coupled map lattice (CML) are not restricted to the problems in spatiotemporal chaos, but include pattern formations, some solid state problems, biological information processing and engineering problems.

Using CML methods, Yanagita simulated pool boiling phenomena and succeeded in explaining the mode of transition from nucleate to film boiling. He assumed that the fundamental dynamics processes of boiling are thermal convection, bubble rising motion and phase change. Although Yanagita's model is very attractive and path-breaking, it deviates some point from the actual boiling process. Firstly, his model permits liquid to evaporate in bulk, a phenomena known as homogeneous nucleation which is different from boiling in usual sense. Secondly, boiling occurs in the Yanagita's model even when the heater surface temperature is lower than the liquid's saturation temperature. This never happens in the actual boiling system. Finally, Yanagita's model fails to capture the rigorous form of film boiling.

Shoji corrected the deficiencies of the model of Yanagita by including nucleation sites on the heater surface and the Taylor instability. [10]

Chapter 3

Methodology

3.1 Modeling

Boiling phenomena occur during the combined transport of energy, momentum, and matter in the two phase flow. In principle, physical transport phenomena are described by the Navier-Stokes equation. However, using the Navier-Stokes equation to simulate boiling processes has a number of drawbacks. First, numerical instability will occur because the boundary of the two phases (Liquid & vapour) is complex and varies in time. Second, because the computations must be done with high precision to avoid numerical instabilities, the amount of CPU time required for the integration of the equation will be very enormous. As a result, the Navier-Stokes equation-based models cannot be utilised to simulate boiling phenomena in a practical sense.

To describe the nature of boiling, there are two categories of models.

1. Models which describe the phenomena quantitatively.
2. Models that are used to help people comprehend conceptual difficulties but don't have to produce a quantitative agreement.

The Navier-Stokes equation should be used to capture the phenomena quantitatively, however as mentioned above, it is difficult to simulate complex transport phenomena. As a result, we must first understand the qualitative nature of boiling using a basic model. Coupled map lattice (CML) is one of the most powerful strategies to represent the qualitative features of dynamical phenomena in spatially extended systems.

A modeling of physical phenomena by CML is based on the following steps. :

- (a) **Take a set of field variables on a lattice:** Many field variables are required to fully describe boiling processes, including temperature, pressure, velocity, and density. Here we are concerned with temperature field $T_{x,y}^t$ on the lattice (x,y) at time ' t ' in order to simplify the model. We lack some information at this point because we haven't taken into account all of the field variables. Other variable which we do not consider here, however are accounted for implicitly by the mapping function.
- (b) **Extract important effects of the phenomena and decompose them into units :** Our dynamics of boiling is decomposed into independent dynamics by diffusion, generation and floating motion of bubbles, and latent heat.
- (c) **Replace each unit by the simplest possible parallel dynamics on the lattice.**

3.2 Thermal Diffusion

When there exist a temperature gradient exist in a medium, thermal diffusion occurs, which is the relative motion of the components of a gaseous mixture or solution. The homogeneity of mixture composition is disturbed by thermal diffusion: the concentration of components in regions with increasing and decreasing temperatures differs. Governing equation, since thermal conduction occurring in fluid, the following governing equation is applicable as a two-dimensional boiling field is simulated.

$$\frac{\partial T}{\partial t} = \alpha \left(\frac{\partial^2 T}{\partial x^2} + \frac{\partial^2 T}{\partial y^2} \right) \quad (3.1)$$

Here α is a positive coefficient called the thermal diffusivity of the medium. The medium assumed to be isotropic and homogeneous. The fluid may exist in the state of either liquid, liquid and vapour, or only vapour, but each fluid lattice contain either liquid or vapour at a given time.

3.3 Numerical Methods

So we need to discretized the above equation because a computer can work with only a finite amount of data, a first step in preparing a mathematical problem for

computer is to discretize the problem by reducing it to finitely many pieces. For pattern - forming systems, there are two widely used strategies for discretizing continuous field. First the Galerkin method, in which a field is expanded in terms of a specified set of basis function and second is finite difference method, in which the value of the function are assumed to be known at a finite set of space-time points. We are using finite difference method. For that we first discretize the domain by dividing into uniform grids. The data quality and simulation duration increases significantly with smaller step size.

Boundary Conditions : A periodic boundary conditions is imposed on both sides of the boiling field, $i = 0$ and $i = N_x - 1$, because it assumed that the heater surface is infinite in x direction and boiling scenario is identical in every grid section. The temperature on the top of the surface ($N_y - 1$) is at 0° C and bottom is heating surface. Boundary is fixed at T_{top} and T_{Bottom} respectively.

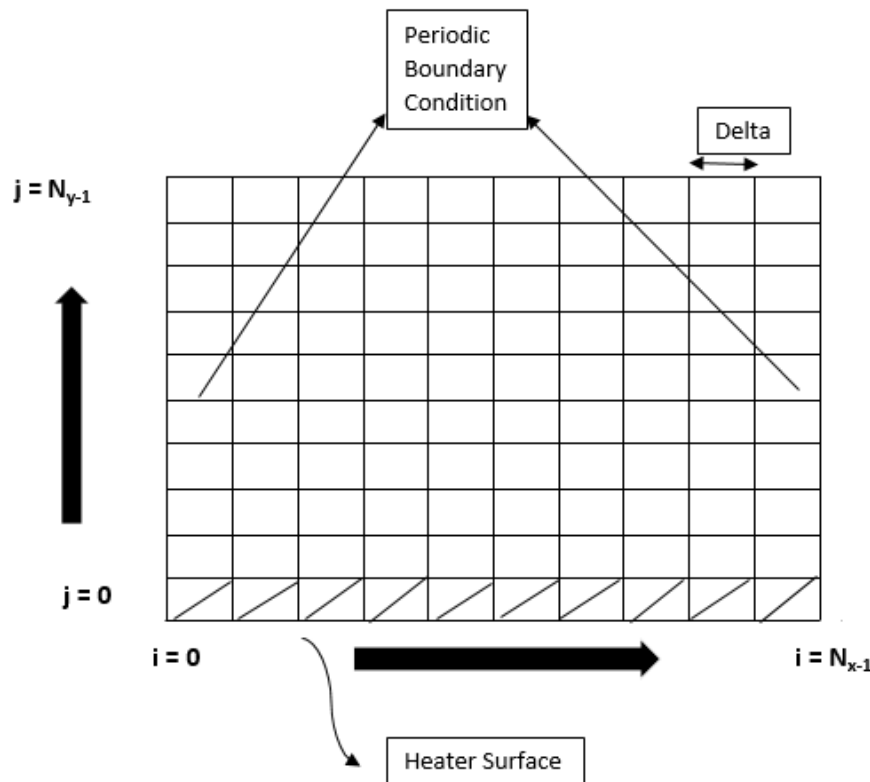


Figure 3.1: Computational Domain and Lattice

Initial Condition : At $t = 0$

$$T_{x,y} = \frac{T_{top} + T_{Bottom}}{2} + \delta$$

where δ is uniform random number.

Discretization Scheme : An explicit finite difference method is used to discretize the governing equation. **appendix A.**

At any interior grid point (i, j) the following equation is valid :

$$T'_{i,j} = T^t_{i,j} + \frac{\epsilon}{4}(T^t_{i+1,j} + T^t_{i,j+1} + T^t_{i-1,j} + T^t_{i,j-1} - 4T^t_{i,j}) \quad (3.2)$$

At the left boundary ($i = 0, j = 1 \rightarrow N_y - 1$) using periodic boundary condition, $T^t_{0,j} = T^t_{N_x-1,j}$ in equation 3.2, gives

$$T'_{0,j} = T^t_{0,j} + \frac{\epsilon}{4}(T^t_{1,j} + T^t_{0,j+1} + T^t_{N_x-1,j} + T^t_{0,j-1} - 4T^t_{0,j})$$

At the right boundary ($i = N_x - 1, j = 1 \rightarrow N_y - 1$) using periodic boundary condition, $T^t_{N_x,j} = T^t_{0,j}$ in equation 3.2, gives

$$T'_{N_x-1,j} = T^t_{N_x-1,j} + \frac{\epsilon}{4}(T^t_{0,j} + T^t_{N_x-1,j+1} + T^t_{N_x-1,j} + T^t_{N_x-1,j-1} - 4T^t_{N_x-1,j})$$

Note that $(-1, j)$ and (N_x, j) are fictitious points outside the computational domain placed at distance of Δx from the left and horizontal boundaries.

Stability : Stability of numerical calculations In forward Euler method following condition should be satisfied.

$$\epsilon = \alpha \left(\frac{\Delta t}{\Delta x^2} + \frac{\Delta t}{\Delta y^2} \right) \leq \frac{1}{2} \quad (3.3)$$

So,

$$\Delta t \leq \frac{1}{2\alpha} \left(\frac{1}{\Delta x^2} + \frac{1}{\Delta y^2} \right)^{-1} \quad (3.4)$$

if $\Delta x = \Delta y = h$

$$\Delta t \leq \frac{h^2}{4} \quad (3.5)$$

3.4 Creation and Floating Motion of Bubbles:

$$\rho(T) = \tanh \alpha(T - T_c) \quad (3.6)$$

The $\rho(T)$ represent generation and floating motion of bubbles. The bubbles float upward by buoyancy which depends upon the inhomogeneity of the density (ρ).

We represent density as $\rho(T) = \tanh \alpha(T - T_c)$, assuming local equilibrium. The phase transition causes an abrupt change in density, which is represented by the hyperbolic tangent.

The bubble motion due to buoyancy and its effect on temperature may be expressed by simply as following mapping.

$$T_{i,j}'' = T_{i,j}' + \frac{\sigma}{2} \{ \rho(T_{i,j+1}') - \rho(T_{i,j-1}') \} \quad (3.7)$$

Equation 3.7 has been derived from the equations of motion and energy mainly driven by the buoyancy force and the horizontal component of velocity and viscous force may be negligibly small. **Appendix B**.

A cell with a temperature greater than T_c is referred to as a bubble, and it is transmitted upward due to the inhomogeneity of the density $\rho(T_{i,j+1}') - \rho(T_{i,j-1}')$. In the continuum limit, equation 3.6 becomes

$$\frac{\partial T}{\partial t} = -\sigma T \frac{\partial \rho}{\partial T} \frac{\partial T}{\partial y}$$

Then the bubble is floating with speed

$$T \frac{\partial \rho}{\partial T} \Big|_{T=T_{bubble}}$$

Where T_{bubble} is mean temperature of bubbles. Rewriting the equation, we obtain,

$$\frac{\partial}{\partial t} \log T = -\sigma \frac{\partial \rho}{\partial T} \frac{\partial T}{\partial y}$$

The growth rate is proportional to heat flux $\frac{\partial T}{\partial y}$

3.5 Latent Heat Effect :

The third procedure represents the latent heat effect. When the phase transition from liquid to gas occurs at a cell, the temperature of its nearest neighbors decreases by following rules:

$$1. \quad T_{x,y}'' > T_c \quad \text{and} \quad T_{x,y}^t < T_c \quad \text{then} \quad T_{n(x,y)}^{t+1} = T_{n(x,y)}'' - \eta$$

$$2. \quad T_{x,y}'' < T_c \quad \text{and} \quad T_{x,y}^t > T_c \quad \text{then} \quad T_{n(x,y)}^{t+1} = T_{n(x,y)}'' + \eta$$

where $\mathbf{n}(\mathbf{x}, \mathbf{y})$ shows nearest neighbors of the position (x, y) .

Heat conduction from the bottom plate controls the bubble generation process. Then we can ignore convective heat transmission. The bubbles that absorb the latent heat in the boiling regime float upward at a faster rate than the fluid's convective motion. Then main part of heat transfer is governed by floating motion of bubbles (the so-called latent heat transfer mechanism). As a result, convection, which is a secondary impact, can be ignored under the boiling regime.

3.6 Parameter Details

Simulation is carried out in two dimensional square domain of grid.

Initialized variable	Value taken for FDM
Size of spatial grid	80×80
Size of uniform random number	80×80
Spatial step size	1
time step size	1
ε	0.5
α	10
σ	0.1
η	0.1
T_c	10

3.7 Time advancement

Time is advanced by repeating a set of mapping the dynamic process (section 3.3 to 3.5) in such a manner that

$$T_{i,j}^t \xrightarrow{\text{Diffusion}} T_{i,j}'' \xrightarrow{\text{Bubble-Motion}} T_{i,j}''' \xrightarrow{\text{Latent-Heat}} T_{(i,j)}^{t+1}$$

where the superscript t and $t + 1$ indicates the present and future values of temperature.

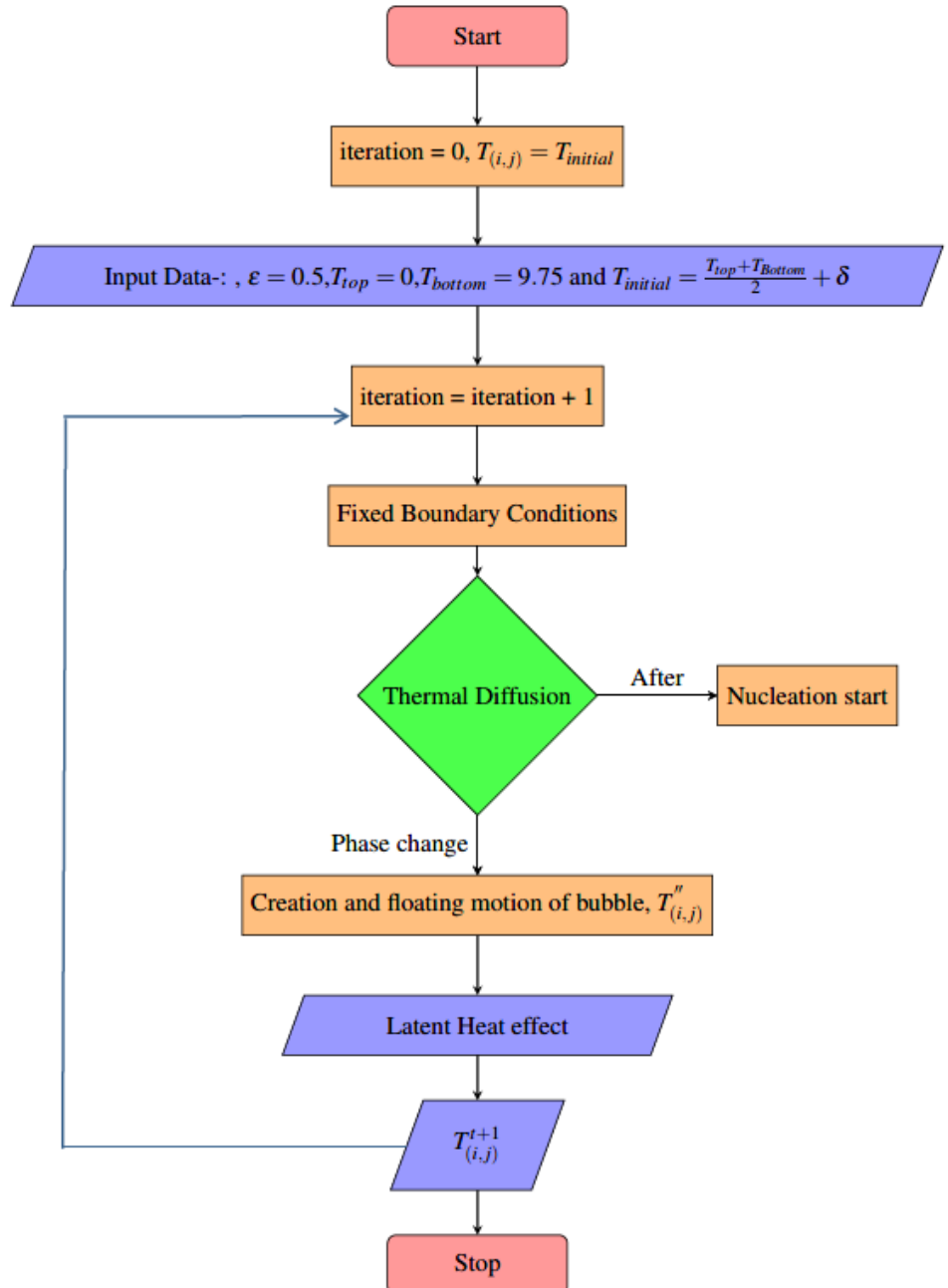
3.8 Overall Solution Algorithm

1. Specify Heater temperature (T_{Bottom}) and cooling temperature (T_{top}) and T^t .

2. Calculate T' by solving the thermal diffusion equation 3.1.
3. Use equation 3.7 to get T'' .
4. Apply nearest neighbour condition specify in section 3.5 and obtain $T_{(i,j)}^{t+1}$.
5. Obtain result for different bottom temperature (T_{Bottom}) and re-specify T^t .
6. STOP.

A concise flowchart of the solution algorithm is shown in following subsection

Flowchart of the overall solution algorithm



Chapter 4

Results and Discussion

We investigated the stationary spatial patterns of this model when the temperature T_{bottom} rises. We found three successive phases.

4.1 Thermal Diffusion Plot

In chapter 3, there has been a mention about the thermal diffusion process. If temperature of bottom plate is below some critical value $T_{B.P.}$ (Boiling Point ≈ 9.77) $< T_{bottom}$ so heat is mainly transported by the diffusion process. (**Figure 4.1**) If the temperature gradient $\Delta T = T_{bottom} - T_{top}$ is sufficiently small, the mean temperature field obeys the Fourier law for the heat conduction.

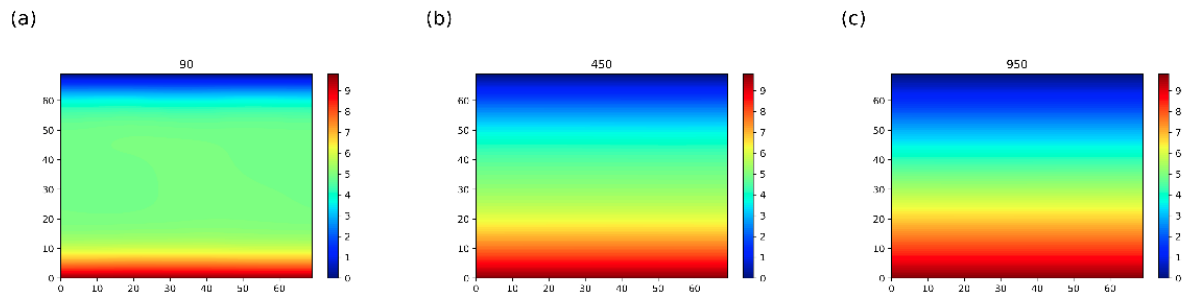


Figure 4.1: Diffusion Plot at time: **a =90, b =450, c =950**

The simulation code in **appendix ??**.

4.2 Creation and floating motion of bubbles

Heat is no longer efficiently transmitted by diffusion above the boiling point $T_{B.P.}$ and a substantial temperature gradient forms near the bottom. Thus the procedure in section 3.4 is relevant and bubbles (i.e. patches where $T > T_c$) appears.

The bubbles do not expand very strongly when they are slightly above the boiling point. The bubbles finally vanish before floating away.

As T_{bottom} increases, bubbles are released from the bottom constantly and the number of bubbles increases. Most of them shrink in size and finally vanish due to thermal diffusion (Figure 4.2 and Figure 4.3). With increasing height y , the mean temperature decreases suddenly (boundary layer appear near the top and the bottom plate), implying that heat is transferred efficiently in boiling regime.

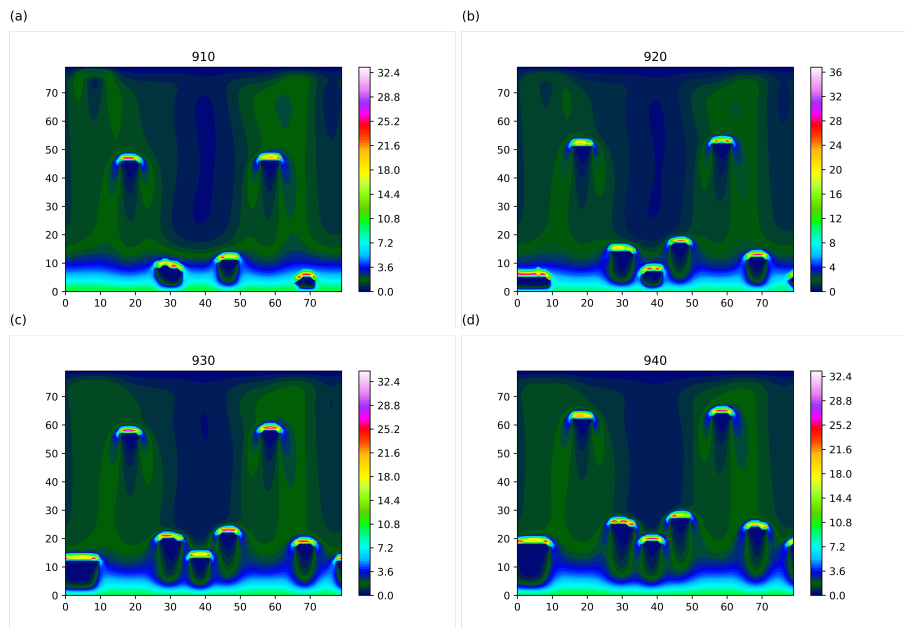


Figure 4.2: $T_{bottom} = 9.75$ at time: **a = 910, b = 920, c = 930, d = 940**

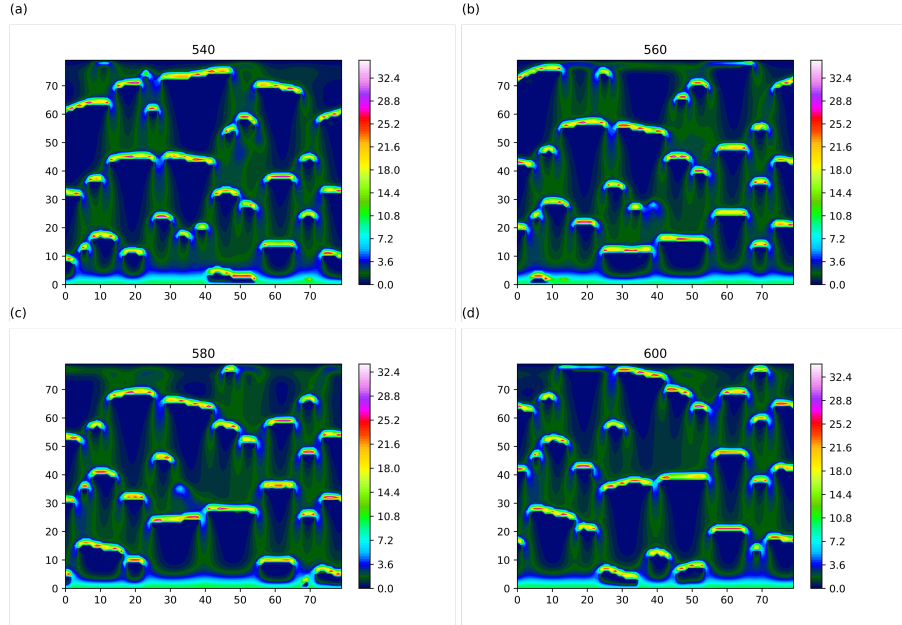


Figure 4.3: $T_{bottom} = 9.85$ at time: **a = 540, b = 560, c = 580, d = 600**

At the burnout point $T_{B,O} \approx 9.92$, bubbles join to form a film vapor. The creation of a patched to striped pattern is visible when the bottom temperature rises. Isolated bubbles begin to merge together over time, large bubbles grow, and eventually a film bubble appears. The film vapour detaches from the bottom plate simultaneously in our model. Thus we observed striped pattern in **Figure. 4.4** and **Figure 4.5**

This pattern is stable because our model does not include hydrodynamic effects. In experiment, we can not observe such a pattern because the hydrodynamic and surface effect play important roles for the shape of bubbles. However, the bubbles which have uniform size are detached from film vapor and are floating upward, because the film vapor which covers the surface of the heater has an unstable mode. This behaviour is remarkably similar to our concept for the striped pattern generation process.

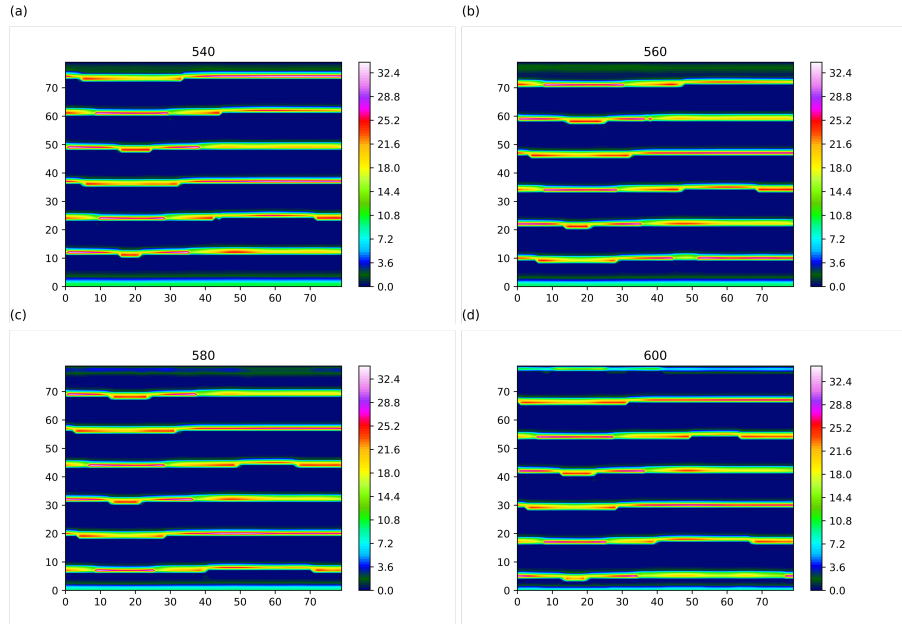


Figure 4.4: $T_{bottom} = 9.92$ at time: **a = 540, b = 560, c = 580,c = 600**

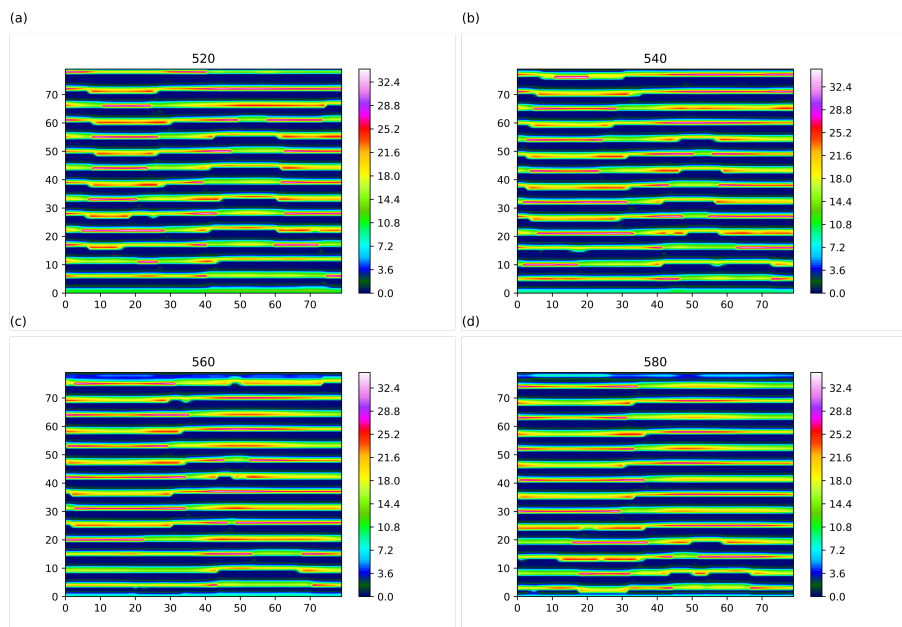


Figure 4.5: $T_{bottom} = 9.96$ at time: **a = 520, b = 540, c = 560,c = 580**

4.3 Heat Flux

Nukiyama used boiling characteristic curve to characterise the boiling transition by measuring the temperature of the heater as a function of the heat flux input into the system. In our simulation, we define the heat flux by

$$Q = \frac{1}{L_x} \left\langle \sum_{x=1}^{L_x} \frac{\sigma}{2} (T_{x,1}^t - T_{bottom}) \right\rangle \quad (4.1)$$

Where L_x is the length of horizontal direction. The heat flux increases from boiling point $T_{B.P.} \approx 9.8$ while it decreases from burnout point $T_{B.O.} \approx 9.92$. Because in our simulations the system has a prescribed top and bottom temperature, we can see the unstable branch where the heat flux is decreasing. **Our model does not reproduce the increasing region DE in Figure. 1.5. Because the heat transfer by convection and radiation play important role in this region.**

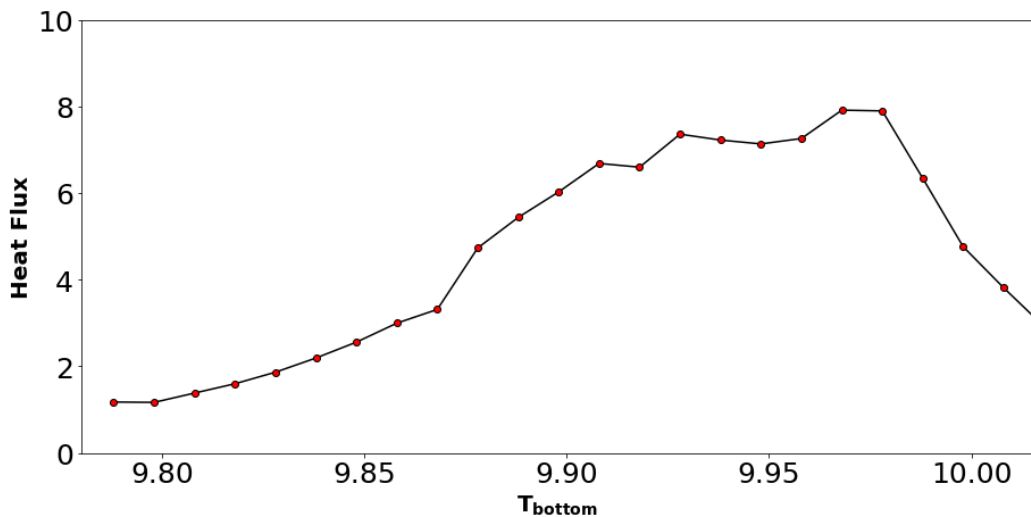


Figure 4.6: T_{bottom} V/S Heat Flux

However, our curve in Figure 4.6 is in qualitative agreement with the experimental observation.

Chapter 5

Conclusions

The boiling transition was never explained by models based on the *Navier-Stokes equation* because the system is too complex to simulate. The present CML study reveals even simple theoretical model for pool boiling. This model shows transition from nucleate to film boiling. Some qualitative aspects of this transition are replicated by the model. In particular, boiling characteristics curve agrees with experimental observation qualitatively.

In constructing a CML model, there is some arbitrariness regarding the determination of the procedures. For example, in our model, we can replace the hyperbolic tangent which represents the dynamics of the phase transition by some other function. However, if the procedure belongs to a universality class, we can actually replace the hyperbolic tangent by a piece-wise linear function, the qualitative feature of the boiling transition does not change. Moreover, the boiling transition is a macroscopic percolative (the movement and filtering of fluids through porous materials) phenomenon for a bubble, it does not depend on the details of the dynamics of the phase transition.

The present model we can extended to reproduce the saturated pool boiling curve for different fluids. Future work may also be done to model pool boiling on three dimensional space, which is more realistic and to investigate the effect of much larger pool heights.

Appendix A

Appendices

A Thermal Diffusion

Thermal Diffusion equation

$$\frac{\partial T}{\partial t} = \alpha \left(\frac{\partial^2 T}{\partial x^2} + \frac{\partial^2 T}{\partial y^2} \right)$$

Numerical Method : One way to solve partial differential equation is to approximate all derivative by finite difference. Hence these equation are computationally solved by the explicit forward difference method. We partition domain in space using a mesh $x_0, x_1, x_2, \dots, x_i$ along x-axis having spatial separation of Δx and $y_0, y_1, y_2, \dots, y_i$ with a separation of Δy . In the same way t also partitioned with separation of Δt . Here we assume uniform partition in both space and time so that the difference between two consecutive points remain same. We can find spatial derivative by perform Taylor series expansion of temperature field around $T_{i+1,j}$ and $T_{i-1,j}$ we can write like this...

$$T_{i+1,j} = T_{i,j} + \frac{\partial T}{\partial x} \Big|_{i,j} \Delta x + \frac{1}{2} \frac{\partial^2 T}{\partial x^2} \Big|_{i,j} \Delta x^2 + \dots \quad (\text{A.1})$$

$$T_{i-1,j} = T_{i,j} - \frac{\partial T}{\partial x} \Big|_{i,j} \Delta x + \frac{1}{2} \frac{\partial^2 T}{\partial x^2} \Big|_{i,j} \Delta x^2 + \dots \quad (\text{A.2})$$

equation A.1 - equationA.2 we get.

$$\frac{\partial T}{\partial x} = \frac{T_{i+1,j} - T_{i-1,j}}{2\Delta x} + \mathcal{O}(\Delta x) \quad (\text{A.3})$$

This equation A.3 known as central difference method. We can also write forward difference method.

$$\frac{\partial T}{\partial x} = \frac{T_{i+1,j} - T_{i,j}}{\Delta x} + \mathcal{O}(\Delta x) \quad (\text{A.4})$$

Then according to finite difference method we can write time derivative also.

$$\frac{\partial T}{\partial t} = \frac{T_{i,j}^{n+1} - T_{i,j}^n}{\Delta t} \quad (\text{A.5})$$

$T_{i,j}^n$ can be denoted as the value of T at the spatial point (x, y) at time t_n .

Similarly we can write second order partial differential equation A.1 + equation A.2 we can get.

$$\frac{\partial^2 T}{\partial x^2} = \frac{T_{i+1,j} - 2T_{i,j} + T_{i-1,j}}{\Delta x^2} + \mathcal{O}(\Delta x) \quad (\text{A.6})$$

Now we can neglect higher order term

$$\frac{\partial T}{\partial x} = \frac{T_{i+1,j} - T_{i,j}}{\Delta x} \quad (\text{A.7})$$

$$\frac{\partial^2 T}{\partial x^2} = \frac{T_{i+1,j} - 2T_{i,j} + T_{i-1,j}}{\Delta x^2} \quad (\text{A.8})$$

Similarly with respect to y

$$\frac{\partial^2 T}{\partial y^2} = \frac{T_{i,j+1} - 2T_{i,j} + T_{i,j-1}}{\Delta y^2} \quad (\text{A.9})$$

We already considered separation in x - direction and y - direction is same so we can write thermal diffusion equation 3.1

$$\frac{T_{i,j}^{n+1} - T_{i,j}^n}{\Delta t} = \alpha \left(\frac{T_{i+1,j} - 2T_{i,j} + T_{i-1,j}}{\Delta x^2} + \frac{T_{i,j+1} - 2T_{i,j} + T_{i,j-1}}{\Delta y^2} \right) \quad (\text{A.10})$$

$$\Delta x = \Delta y$$

equation become

$$T_{i,j}^{n+1} = T_{i,j}^n + \epsilon (T_{i+1,j} + T_{i-1,j} + T_{i,j+1} - 4T_{i,j} + T_{i,j-1}) \quad (\text{A.11})$$

$$\epsilon = \frac{\alpha \Delta t}{\Delta x^2}$$

B Creation and floating motion of Bubbles

Assumptions.

1. No horizontal component of velocity, i.e. $u = 0, V = v\hat{j}$

2. Inviscid flow, i.e. $\nu = 0$ (The viscosity of a fluid is equal to 0 in an inviscid fluid.)

3. Ideal gas equation is valid for the fluid, ideal gas equation $p = \rho RT$

where ' p ' is pressure, ' ρ ' is the density of fluid and ' R ' is gas constant and ' T ' is temperature of the fluid.

Continuity Equation.

$$\frac{\partial u}{\partial x} + \frac{\partial v}{\partial y} = 0 \quad (\text{A.12})$$

Here, ' ρ ' is constant except in the y-momentum equation and $u = 0$. equation A.12 reduces to $\frac{\partial v}{\partial y} = 0$. Hence $v = \text{constant}$ in y-direction.

Momentum Equations. x - momentum are neglected, y - momentum equation :

$$\rho \left(\frac{\partial v}{\partial t} + u \frac{\partial v}{\partial x} + v \frac{\partial v}{\partial y} \right) = Y - \frac{\partial p}{\partial y} + \nu \left(\frac{\partial^2 v}{\partial x^2} + \frac{\partial^2 v}{\partial y^2} \right) \quad (\text{A.13})$$

Since $u = 0$ and $\frac{\partial v}{\partial y} = 0$ and $v = 0$, so eq. A.13 reduces to

$$\rho \frac{\partial v}{\partial t} = Y - \frac{\partial p}{\partial y} \quad (\text{A.14})$$

Energy Equation. Thermal Diffusion has already been considered in the first map and hence the diffusion term in the right hand side term is not appearing here.

$$\frac{\partial T}{\partial t} + u \frac{\partial T}{\partial x} + v \frac{\partial T}{\partial y} = 0 \quad (\text{A.15})$$

Since $u = 0$ energy equation reduce to

$$\frac{\partial T}{\partial t} + v \frac{\partial T}{\partial y} = 0 \quad (\text{A.16})$$

Now in equation A.14 , $Y = -\rho g$ (here, y is positive upward and "g" is acting downward)

$$\frac{\partial p}{\partial y} = -\rho_\infty g$$

where ρ_∞ is bulk density of fluid. Substituting "Y" and $\frac{\partial p}{\partial y}$ in equation A.14.

$$\begin{aligned} \rho \frac{\partial v}{\partial t} &= -\rho g - (-\rho_\infty g) \\ \frac{\partial v}{\partial t} &= \frac{g}{\rho} (\rho_\infty - \rho) \end{aligned} \quad (\text{A.17})$$

Assuming ρ v/s T linearly varying in the small temperature range,

$$\frac{\rho_\infty - \rho}{T_\infty - T} = \frac{\partial \rho}{\partial T}$$

$$\rho_\infty - \rho = T_\infty - T \frac{\partial \rho}{\partial T}$$

putting the value of $(\rho_\infty - \rho)$ in equation A.17, we get

$$\frac{\partial v}{\partial t} = \frac{g}{\rho} \frac{\partial \rho}{\partial T}$$

Using the explicit finite difference method (note that superscript ' refers to thermal diffusion map and bubble rising velocity is zero at that time)

$$\begin{aligned} \frac{v - 0}{\Delta t} &= \frac{g}{\rho} \frac{\partial \rho}{\partial T} \\ v &= \frac{g}{\rho} \frac{\partial \rho}{\partial T} (T_\infty - T'_{i,j}) \Delta t \end{aligned} \quad (\text{A.18})$$

from equation A.16, $\frac{\partial T}{\partial t} = -v \frac{\partial T}{\partial y}$. Substituting the expression for "v" in eq. A.18

$$\begin{aligned} \frac{\partial T}{\partial t} &= \frac{g}{\rho} \frac{\partial \rho}{\partial T} (T_\infty - T'_{i,j}) \Delta t \frac{\partial T}{\partial y} \\ \frac{\partial T}{\partial t} &= \frac{g}{\rho} (T_\infty - T'_{i,j}) \Delta t \frac{\partial \rho}{\partial y} \end{aligned}$$

We can also write as

$$\boxed{\frac{\partial T}{\partial t} = \frac{g}{\rho} (T_\infty - T'_{i,j}) \Delta t \frac{\partial \rho}{\partial T} \frac{\partial T}{\partial y}} \quad (\text{A.19})$$

$$\boxed{\frac{\partial T}{\partial t} = -\sigma T \frac{\partial \rho}{\partial T} \frac{\partial T}{\partial y}} \quad (\text{A.20})$$

Using the explicit finite difference method.

$$\begin{aligned} \frac{T''_{i,j} - T'_{i,j}}{\Delta t} &= -\frac{g}{\rho} (T_\infty - T'_{i,j}) \Delta t \frac{\partial \rho}{\partial y} \\ T''_{i,j} &= T'_{i,j} - \frac{g}{\rho} (T_\infty - T'_{i,j}) (\Delta t)^2 \frac{\partial \rho}{\partial y} \\ T''_{i,j} &= T'_{i,j} - \frac{g}{\rho} (T_\infty - T'_{i,j}) (\Delta t)^2 \left(\frac{\rho_{i,j+1} - \rho_{i,j-1}}{2\Delta y} \right) \\ T''_{i,j} &= T'_{i,j} - \frac{g}{2} \left(\frac{T_\infty - T'_{i,j}}{\Delta y} \right) (\Delta t)^2 \left(\frac{\rho_{i,j+1} - \rho_{i,j-1}}{\rho} \right) \end{aligned}$$

We know $\rho = \frac{p}{RT}$

$$T_{i,j}'' = T_{i,j}' - \frac{g}{2} \left[\frac{T_\infty - T_{i,j}'}{\Delta y} \right] \frac{RT_{i,j}'}{p} (\Delta t)^2 (\rho_{i,j+1} - \rho_{i,j-1})$$

Assuming $p = p_{sat} = constant = \rho_{sat}RT_{sat}$

$$T_{i,j}'' = T_{i,j}' - \frac{g}{2} \left[\frac{(T_\infty - T_{i,j}')(\Delta t)^2}{\Delta y} \right] \frac{T_{i,j}'}{\rho_{sat}T_{sat}} (\rho_{i,j+1} - \rho_{i,j-1})$$

$T_{i,j}'' = T_{i,j}' - \frac{\sigma}{2} T_{i,j}' (\rho_{i,j+1} - \rho_{i,j-1})$

(A.21)

where $\sigma = \frac{g}{2} \left[\frac{(T_\infty - T_{i,j}')(\Delta t)^2}{\Delta y} \right] \frac{1}{\rho_{sat}T_{sat}}$

References

- [1] MC Cross and PC Hohenberg. “Spatiotemporal chaos”. In: *Science* 263.5153 (1994), pp. 1569–1570.
- [2] Amir Faghri and Yuwen Zhang. *Transport phenomena in multiphase systems*. Elsevier, 2006.
- [3] PS Ghoshdastidar, S Kabelac, and A Mohanty. “Numerical modelling of atmospheric pool boiling by the coupled map lattice method”. In: *Proceedings of the Institution of Mechanical Engineers, Part C: Journal of Mechanical Engineering Science* 218.2 (2004), pp. 195–205.
- [4] Kunihiko Kaneko. “Overview of coupled map lattices”. In: *Chaos: An Interdisciplinary Journal of Nonlinear Science* 2.3 (1992), pp. 279–282.
- [5] Kunihiko Kaneko. “Spatiotemporal chaos in one-and two-dimensional coupled map lattices”. In: *Physica D: Nonlinear Phenomena* 37.1-3 (1989), pp. 60–82.
- [6] Edward N Lorenz. “Deterministic nonperiodic flow”. In: *Journal of atmospheric sciences* 20.2 (1963), pp. 130–141.
- [7] S. Rajasekar M. Lakshmanan. *Nonlinear dynamics Integrability, Chaos, and Patterns*. Springer-Verlag Berlin Heidelberg, 2003.
- [8] Robert M May. “Simple mathematical models with very complicated dynamics”. In: *The Theory of Chaotic Attractors* (2004), pp. 85–93.
- [9] Nukiyama S. “Maximum and minimum values of heat transmitted from metal to boiling water under atmospheric pressure”. In: *Journal of Society of Mechanical Engineers, Japan* 37.1-3 (1934), p. 367.
- [10] M Shoji. “Boiling Simulator, A Simple Theoretical Model of Boiling”. In: *KN paper ICMF 98, Lyon* (1998).
- [11] Wikipedia. “Leiden Effect”. In: (2013). [Online; accessed June 10, 2022]. URL: https://en.wikipedia.org/wiki/Leidenfrost_effect.

- [12] Tatsuo Yanagita. “Phenomenology of boiling: A coupled map lattice model”. In: *Chaos: An Interdisciplinary Journal of Nonlinear Science* 2.3 (1992), pp. 343–350.
- [13] Tatsuo Yanagita and Kunihiko Kaneko. “Coupled map lattice model for convection”. In: *Physics Letters A* 175.6 (1993), pp. 415–420.